

# Magnetostatic fields in tubular nanostructures

P Landeros<sup>1</sup>, P R Guzmán<sup>2</sup>, R Soto-Garrido<sup>3</sup> and J Escrig<sup>4,5</sup>

<sup>1</sup> Departamento de Física, Universidad Técnica Federico Santa María, Avenida España 1680, Casilla 110 V, 2340000 Valparaíso, Chile

<sup>2</sup> Departamento de Matemática, Universidad Técnica Federico Santa María, Avenida España 1680, Casilla 110 V, 2340000 Valparaíso, Chile

<sup>3</sup> Department of Physics, University of Illinois at Urbana-Champaign, 1110 W. Green Street, Urbana, 61801 IL, USA

<sup>4</sup> Departamento de Física, Universidad de Santiago de Chile (USACH), Avenida Ecuador 3493, 917-0124 Santiago, Chile

<sup>5</sup> Centro para el Desarrollo de la Nanociencia y Nanotecnología, CEDENNA, 917-0124 Santiago, Chile

E-mail: [pedro.landeros@usm.cl](mailto:pedro.landeros@usm.cl)

Received 1 September 2009, in final form 4 October 2009

Published 30 October 2009

Online at [stacks.iop.org/JPhysD/42/225002](http://stacks.iop.org/JPhysD/42/225002)

## Abstract

The non-uniform magnetostatic field produced by the equilibrium and non-equilibrium magnetic states of magnetic nanotubes has been investigated theoretically. We consider magnetic fields produced by actual equilibrium states and transverse and vortex domain walls confined within the nanostructure. Our calculations allow us to understand the importance of the magnetostatic field in nanomagnetism, which is frequently considered as a uniform field. Moreover, our results can be used as a basis for future research of other properties, such as the investigation of spin waves when domain walls are present, or the motion of a magnetic particle near a magnetic field.

(Some figures in this article are in colour only in the electronic version)

## 1. Introduction

Structures of nanometric dimensions are strongly dependent on size and shape, mainly due to the fact that the characteristic scales of many physical phenomena are comparable to the dimensions of current nanostructures. Magnetism makes no exception and fundamental research of nanomagnets is further fuelled by their prospective applications in technological devices [1, 2] and biomedical applications [3, 4]. The implementation of nanomagnets into potential devices requires a deep control of their physical properties; hence it is very important to control the shape and size of the nanoparticles which are crucial to determine their magnetic properties. Within currently available nanostructures, nanotubes made from 3d transition metals and their alloys are of particular importance, since the nanotube topologies provide us with two surfaces for modification, allowing the generation of multifunctional magnetic nanoparticles. Clearly, a technology capable of modifying different surfaces would be highly desirable [5].

Recently hollow tubular nanostructures have been synthesized [6–9] and may be useful for applications in biotechnology, because low density magnetic nanotubes (MNs) can float in solutions and are more suitable for *in vivo* applications [5]. The magnetism of planar and circular nanowires has been intensely investigated, while MNs have received less attention, although MNs do not exhibit magnetic vortex cores or Bloch points [10], leading to different behaviour with a more controllable reversal process.

It is well known that changes in the cross section of the MNs strongly affect the reversal mechanism and the overall magnetic behaviour [8, 11–14]. Recent papers have shown that MNs present three main equilibrium states: a uniform state (U), a mixed state (M) and a vortex state (V). On the basis of theoretical models it has been argued that for nanotubes with an outer radius of less than  $4L_x$  (where  $L_x = \sqrt{2A/\mu_0 M_s^2}$  is the exchange length,  $M_s$  is the saturation magnetization and  $A$  is the stiffness constant of the magnetic material) the magnetization is almost uniform and oriented principally along the cylindrical axis [14]. We call this configuration

the uniform state. Also, for nanotubes with  $R \gtrsim 4L_x$  the magnetic equilibrium state corresponds to the so-called mixed state, which is a mixture of U and V states [8, 14–16]. This state presents a uniform magnetization along the middle region of the tube, and near the lower and upper surfaces the magnetization deviates from uniformity in order to reduce the magnetostatic field [14]. Finally, there is a transition from the M state to the vortex state as can be seen from figure 7 of [14].

On the other hand, it has been argued that domain wall propagation in nanostructures, which can be achieved by external fields or spin-currents, is of basic scientific and technological interest [17, 18]. More recently, it has been shown that the size-dependent reversal process in MNs occurs via DW nucleation and subsequent DW propagation. The DW microstructure depends on the tube cross section and can be a transverse wall (TW) for tube radius ( $R$ ) smaller than a critical radius ( $R_c(\beta)$ ), or a vortex wall (VW) for  $R > R_c(\beta)$  [19–22], where  $\beta \equiv R_i/R$  is the ratio between the inner ( $R_i$ ) and outer tube radii. The critical radius defined above depends on the magnetic material and on the shape factor  $\beta$  and then it can be tailored manipulating the geometrical parameters. In polycrystalline systems, the critical radius,  $R_c(\beta)$ , ranges from a few nanometres to 20 nm approximately, and therefore, since experimentally fabricated MNs satisfy  $R > R_c(\beta)$ , we can expect that the propagation of a vortex DW is the dominant magnetization reversal mechanism for ferromagnetic nanotubes [19–22].

Although the magnetostatic field of MNs with uniform magnetization has already been investigated [23–25], an analytical model for the magnetostatic field produced by a MN with the above mentioned configurations, either equilibrium or transient states, has not yet been performed. Our intention is to fill this gap by using simple magnetization models [14, 19]. Since nanostructures are usually polycrystalline, the crystallographic orientations of the crystallites are random and, as a consequence, the average magnetic anisotropy of the particle is very small. In view of that, it will be neglected in our calculations [26, 27]. This paper is organized as follows: In section 2 we present the magnetization models, including in section 2.1 the equilibrium states M and U and the VW, and then in section 2.2 we discuss the case of the TW. Results and discussions are summarized in section 3 and conclusions in section 4.

## 2. Calculation of the magnetostatic fields

In this section we present explicit expressions to evaluate the magnetostatic field for nanotubes with the magnetization states described above. Within the continuum theory of ferromagnetism [28], the magnetostatic field is given by  $\mathbf{H} = -\nabla U$ , where  $U$  is the magnetostatic potential, which depends on the magnetization itself. The basic assumption we address in this paper is that the nanotubes we are considering are thin enough to avoid any dependence of the magnetization on the radial coordinate. In what follows we present the magnetization and the related magnetostatic field for the equilibrium states (U and M) and both DW structures aforementioned.

### 2.1. Equilibrium states and vortex-like configurations

First, we consider nanotubes with vortex-like configurations, as the mixed state and the transient state with a VW confined within the tube. The magnetization of such magnetic configurations can be generally written as  $\mathbf{M}(z) = M_s \mathbf{m}(z) = M_s(m_\phi(z)\hat{\phi} + m_z(z)\hat{z})$ , where  $m_z(z) = \cos \Theta(z)$  and  $m_\phi(z) = \sin \Theta(z)$ , with  $\Theta(z)$  being the angle between the local magnetization vector and the cylindrical  $z$ -axis. With this rather general form for the magnetization we can compute the magnetostatic field produced by  $\mathbf{M}(z)$ . Following the calculations of [14], the magnetostatic potential can be written as

$$U(\rho, z) = \frac{M_s}{2} \int_0^\infty g(q) J_0(q\rho) [f_s + f_v] dq, \quad (1)$$

where  $f_s$  and  $f_v$  come from the surface and volumetric magnetic charges and can be written as

$$f_s \equiv -m_z(0)e^{-q|z|} + m_z(L)e^{-q|z-L|}, \quad (2)$$

$$f_v \equiv -\int_0^L \frac{\partial m_z(y)}{\partial y} e^{-q|z-y|} dy. \quad (3)$$

In the potential we have also defined

$$g(q) \equiv (R/q)[J_1(qR) - \beta J_1(\beta qR)], \quad (4)$$

where  $J_m(x)$  are Bessel functions. The magnetostatic field associated with the above potential can be written as  $\mathbf{H} = -\nabla U(\rho, z)$ , and then, the cylindrical components of the field are  $H_\phi = 0$ ,

$$H_\rho = \frac{M_s}{2} \int_0^\infty q g(q) J_1(q\rho) [f_s + f_v] dq, \quad (5)$$

$$H_z = -\frac{M_s}{2} \int_0^\infty g(q) J_0(q\rho) \left[ \frac{\partial f_s}{\partial z} + \frac{\partial f_v}{\partial z} \right] dq. \quad (6)$$

At this point we are in a position to calculate the magnetostatic field through the reversal process for MNs, as well as to investigate the changes in the magnetostatic field when the equilibrium state is properly considered. In what follows we will use the equations above to calculate the magnetostatic field for the M state and the vortex DW.

**2.1.1. Equilibrium magnetization states.** The arrangement of magnetic moments in a MN with small radius can be seen as a uniform state in the middle region of the tube, but with vortex-like deviations of the magnetization located at the tube ends [8, 14–16]. This mixed state has been observed by micromagnetic simulations [8, 15, 16] and studied theoretically [14]. It has been shown that the two equilibrium states can be studied with the model for the M state. In other words, the U state is a special case of the former, as we will see later. The model that we have used for the M state is given by the function [14]

$$\Theta(z) = \begin{cases} \theta_0(d-z)/d & \text{for } 0 \leq z \leq d \\ 0 & \text{for } d \leq z \leq L - \lambda \\ \theta_L(z - L + \lambda)/\lambda & \text{for } L - \lambda \leq z \leq L, \end{cases} \quad (7)$$

where  $d$  and  $\lambda$  are the dimensions of the regions where the magnetization deviates from the  $z$ -axis. In the model,  $\theta_0$  and  $\theta_L$  correspond to angles between the magnetization and the  $z$ -axis evaluated at the tube ends. Note that we obtain the uniform magnetization state in the limit  $m_z(0) = m_z(L) = 1$  ( $\theta_0 = \theta_L = 0$ ) which occurs approximately for a radius smaller than  $4L_x$  [14]. The parameters of the model are such that they minimize the total energy for each set of geometrical parameters. For simplicity we consider symmetric nanotubes, which are tubes with no difference between both tube ends. In those cases the four-parameter ( $d, \lambda, \theta_0, \theta_L$ ) variational problem is reduced to a two-parameter variational problem, when  $d = \lambda$  and  $\theta_0 = \theta_L$  [14]. Then,  $f_s$  and  $f_v$  become

$$f_s^M = \cos \theta_0 (-e^{-q|z|} + e^{-q|z-L|}), \quad (8)$$

$$f_v^M = \frac{\theta_0}{d} \int_0^d \sin \left( \theta_0 \frac{d-y}{d} \right) [e^{-q|z+y-L|} - e^{-q|z-y|}] dy. \quad (9)$$

With these quantities in hand we can compute the magnetostatic field  $\mathbf{H}(\rho, z)$  at any point. Also, the uniform magnetization state is recovered with  $\theta_0 = 0$ , where the functions reduce to  $f_s^U = -e^{-q|z|} + e^{-q|z-L|}$ ,  $f_v^U = 0$ .

**2.1.2. Vortex domain wall.** The magnetization of the VW in a nanotube can be expressed in a similar way to the magnetization of the mixed state, that is  $\mathbf{M}(z) = M_s \sin \Theta(z) \hat{\phi} + M_s \cos \Theta(z) \hat{z}$ , but now

$$\Theta^{\text{VW}}(z) = \begin{cases} 0 & \text{for } 0 \leq z \leq z_w - \frac{w}{2} \\ \frac{\pi}{w}(z - z_w) + \frac{\pi}{2} & \text{for } z_w - \frac{w}{2} \leq z \leq z_w + \frac{w}{2} \\ \pi & \text{for } z_w + \frac{w}{2} \leq z \leq L, \end{cases} \quad (10)$$

as presented in [19]. Here  $z_w$  is the location of the centre of the VW, and  $w$  is the wall width. Within the above model, the magnetostatic field can also be expressed with equations (7) and (8), but now the functions  $f_s$  and  $f_v$  become

$$f_s^{\text{VW}} = -e^{-q|z|} - e^{-q|z-L|}, \quad (11)$$

$$f_v^{\text{VW}} = \frac{\pi}{w} \int_{z_w - \frac{w}{2}}^{z_w + \frac{w}{2}} \cos \left( \pi \frac{y - z_w}{w} \right) e^{-q|z-y|} dy. \quad (12)$$

## 2.2. Transverse domain wall

The magnetization of the TW in a nanotube can be expressed in a similar way to the VW, but with  $\mathbf{M}(z) = M_s \sin \Theta(z) \hat{x} + M_s \cos \Theta(z) \hat{z}$  [19], and  $\Theta(z)$  being the same as for the VW. It can be noted that the main difference between VWs and TWs (in nanotubes) is the direction of the in-plane magnetization, and then the nature of the domain wall properties should be different. The model that we use for the TW [19] leads us to understand some basic properties, such as the DW width or the energy barrier for the reversal process. Here we are interested in the visualization of the magnetostatic field produced by a static domain wall. It can be shown that this field can be written as  $\mathbf{H} = -\nabla U(\rho, \phi, z)$ , without the usual axial symmetry of vortex-like states. The case of a VW presents a

magnetostatic potential independent of the angular coordinate  $\phi$ , which secures angular symmetry. Following [19], the field can be written as  $\mathbf{H}^{\text{TW}} = H_\rho^{\text{TW}} \hat{\rho} + H_\phi^{\text{TW}} \hat{\phi} + H_z^{\text{TW}} \hat{z}$ . Provided the magnetostatic potential of the TW can be written as

$$U^{\text{TW}} = U^{\text{VW}} + A(\rho, z) \cos \phi, \quad (13)$$

the components of the magnetostatic field created for the TW can then be expressed as

$$H_\rho^{\text{TW}}(\rho, \phi, z) = H_\rho^{\text{VW}}(\rho, z) + \frac{\partial A(\rho, z)}{\partial \rho} \cos \phi, \quad (14)$$

$$H_\phi^{\text{TW}}(\rho, \phi, z) = -A(\rho, z) \sin \phi, \quad (15)$$

$$H_z^{\text{TW}}(\rho, \phi, z) = H_z^{\text{VW}}(\rho, z) + \frac{\partial A(\rho, z)}{\partial z} \cos \phi, \quad (16)$$

where

$$A(\rho, z) = \frac{M_s}{2} \int_0^\infty qg(q) J_1(q\rho) \zeta(z, q) dq, \quad (17)$$

and

$$\zeta(z, q) \equiv \int_0^L m_x(z') e^{-q|z-z'|} dz'. \quad (18)$$

Here,  $m_x(z) = \sin \Theta^{\text{TW}}(z)$ , with  $\Theta^{\text{TW}}(z) = \Theta^{\text{VW}}(z)$ . The function  $\zeta(z, q)$  possesses the information about the DW microstructure and can be straightforwardly integrated. Finally, note that the widths of the vortex and TWs are essentially different, and should be evaluated within the framework presented in [19].

## 3. Results and discussion

In the above sections we have obtained explicit expressions to calculate the magnetostatic field for different magnetic states in nanotubes. In what follows we present plots of the magnetostatic field produced by the magnetic states relevant to the nanotubes. We begin the discussion with the equilibrium states (U and M) and then analyze the case of vortex and TWs propagating along the nanostructure.

### 3.1. Vector plots of the equilibrium states

As mentioned earlier, the uniform magnetization state ( $\theta_0 = 0$ ) is a special case of the mixed state ( $\theta_0 > 0$ ), and occurs when the tube radius is approximately less than  $4L_x$ , provided the exchange energy dominates over the dipolar one [14]. When  $R > 4L_x$  the magnetization at the tube ends is not entirely parallel to the cylindrical  $z$ -axis; instead it develops vortex domains at the ends in order to reduce the dipolar energy [14]. The long-range character of the dipolar interaction makes the dipolar energy grow as  $N^2$ , whereas the exchange energy grows as  $N$ , with  $N$  the number of atomic magnetic moments in the tube. Therefore, the edge vortex domains increase in size with the radius. In the language of the above equations, the size of the vortex domains is given by the parameters  $\theta_0$  and  $d$ . As  $R$  increases over  $4L_x$ ,  $\theta_0$  and  $d$  increase, as the reader can see from figures 5 and 6 in [14]. To calculate the magnetostatic field we need to know the set of parameters ( $\theta_0, d$ ) which minimize the

**Table 1.**  $(\theta_0, d)$  for MNs with  $\beta = 0.9$  and  $L = 1000L_x$  as a function of their radius.

$R/L_x$	$\theta_0$	$d/L_x$
4	0	—
6	48.7	15.5
10	75.2	41
20	83.3	202.6
27	83.8	414.3

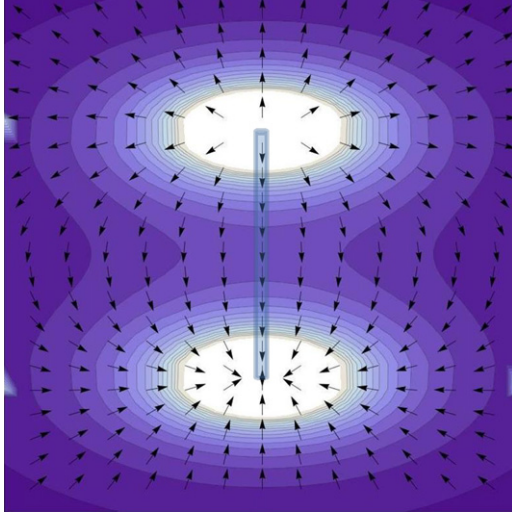


**Figure 1.** Magnetostatic field produced by a tube with uniform magnetization along the symmetry axis. The arrows have been normalized to the local strength of the field. White regions indicate that the field is stronger. Parameters are indicated in the text. (Colour online.)

total energy of the mixed state. Using the expressions for the total energy of [14], we obtain for nanotubes with  $\beta = 0.9$  and  $L = 1000L_x$  different values of  $(\theta_0, d)$  depending on their radius. These results are summarized in table 1. Note that for  $L = 1000L_x$  the transition to a flux-closure vortex state occurs approximately at  $R \approx 27L_x$  [14].

The arrows in figure 1 show the normalized magnetostatic field for a uniformly magnetized MN with  $R = 4L_x$ . The colour code indicates the strength of the field at each point; white indicates that the magnetostatic field is stronger at the tube ends because ‘magnetic charges’ ( $\sigma_M$ ) reside only at the surfaces such that  $\sigma_M = M \cdot \hat{n} \neq 0$ , with  $\hat{n}$  a unit vector normal to the surface of the sample [28]. Provided that the U and M states (as well as the VW) can be represented with  $M = M_\phi(z)\hat{\phi} + M_z(z)\hat{z}$ , it follows that the surface magnetic charges are given by  $\sigma_M(z) = M_z(z)\hat{z} \cdot \hat{n}$ , where  $z = 0$  or  $L$ . In the upper surface of the tube ( $z = L$ )  $\hat{n} = \hat{z}$  and then  $\sigma_M(L) = M_z(L)$ , whereas in the lower surface  $\hat{n} = -\hat{z}$  and  $\sigma_M(0) = -M_z(0)$ . If the actual equilibrium state is the U or the M state, we find positive magnetic charges ( $\sigma_M(L) > 0$ ) located at the upper surface, and this region behaves like a source of charges, as in figure 1; in elementary electromagnetism the field lines emanate from positive charges. Conversely, in the lower surface  $\sigma_M(0) < 0$  and the region behaves like a sink of charge (the field lines converge to these points). It can be shown that for nanotubes in the mixed state, the dipolar field looks very similar to the

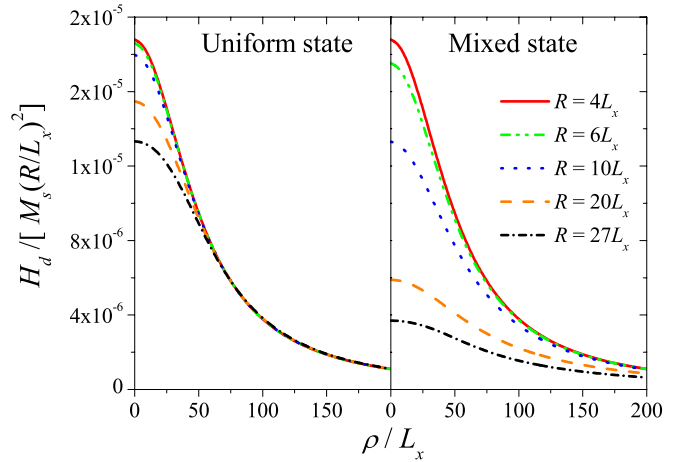


**Figure 2.** Magnetostatic field strength as a function of the radial coordinate and  $z = 1050L_x$ . The left panel shows curves for the uniform state and the right panel shows the magnetostatic field for the mixed state. Different curves represent different tube radii, as depicted in the figure, and parameters have been taken from table 1. (Colour online.)

one plotted in figure 1. As a consequence, we do not present the same plots for tubes in the mixed state, instead we show in figure 2 the dependence of the magnitude of the dipolar field ( $H_d = \sqrt{H_\rho^2 + H_z^2}$ ) on the radial coordinate for different tube radii and  $z = 1050L_x$  (just  $50L_x$  above the upper surface of the tube). We have normalized all the curves to  $M_s(R/L_x)^2$ , and in order to note the difference between the U state and the M state, we present groups of curves for both states.

We observe that a proper consideration of the equilibrium state reduces considerably the dipolar field. This effect becomes critical as the tube radius is increased, which increases the size of the vortex domains of the mixed state [14]. It is worth emphasizing the importance of the proper consideration of the actual magnetic state in tubular nanostructures. For the sake of simplicity, it is a very common practice in magnetism to approximate the magnetization as a uniform field, even though uniform magnetization can be achieved (at zero applied field) only in nanostructures with dimensions of the order of the exchange length [29, 30], or when the nanoparticle is an ellipsoid with the appropriate size. Moreover, cylindrical magnetic nanowires and nanotubes are frequently considered as infinite structures, and only in this limit does the approximation of a uniform dipolar field become plausible, because the cylindrical nanostructures can be considered as ellipsoids only if they are infinitely long. However, actual magnetic nanostructures are not infinite and finite size effects can be relevant. It is well known that the dipolar field produced by a nanoparticle with an ellipsoidal shape is uniform if its size is below the single domain limit (in the absence of an external field) [28]. Within this limit one can safely write the magnetostatic field in terms of the corresponding demagnetizing factor:  $H_d = -NM$ .

The difference between uniform and non-uniform dipolar fields is illustrated in figure 3, where we have plotted  $H_z$ , the component of the magnetostatic field along the tube axis, as a function of  $z$  for different tube radii and magnetic states.

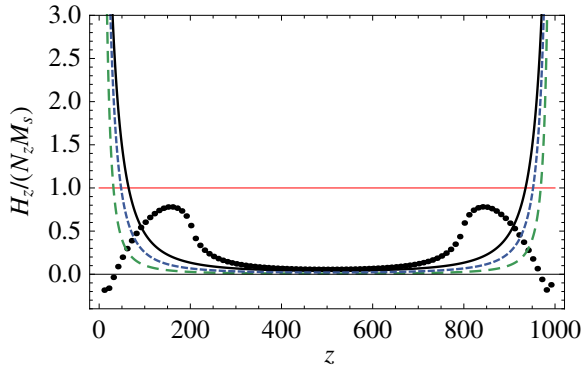


**Figure 3.** Component of the dipolar field along the MN axis as a function of coordinate  $z$ . The fields have been normalized to  $N_z M_s$ , where  $N_z$  is the corresponding demagnetizing factor. The long dashed line corresponds to the U state for  $R/L_x = 4$ . The short dashed line corresponds to the U state and  $R/L_x = 10$ . The thick solid line corresponds to U state and  $R/L_x = 20$  whereas the circles correspond to the M state for  $R/L_x = 20$ . The horizontal line illustrates the strength of the dipolar field calculated in the usual ellipsoid-like approximation for uniform magnetization:  $H_d = -N_z M_s$ . (Colour online.)

The horizontal solid line depicts the strength of the (uniform) dipolar field ( $N_z M_s$ ) produced by an infinite MN with uniform magnetization, whereas the long dash, short dash and solid lines correspond to the field produced by a MN with a uniform magnetization state with radius  $R/L_x = 4, 10$  and  $20$ , respectively. The circles correspond to the dipolar field produced by a MN with a mixed state rather than the incorrect uniform magnetization state, and with  $R/L_x = 20$ . The fields have been normalized to  $N_z M_s$ , where  $N_z = N_z(R, L, \beta)$  is the corresponding demagnetizing factor for a nanotube [12, 31].

### 3.2. Vector plots for a VW

In order to illustrate the basic characteristics of the magnetostatic field produced by a MN with a vortex domain wall, we have chosen nanotubes with  $\beta = 0.9$ ,  $L = 1000L_x$  and  $R = 10L_x$ . Following a previous work realized by some of us [19], we can calculate numerically the DW width ( $w$ ) by minimizing the total energy including the exchange contribution. It is found that  $w = w(\beta, R)$ , and for the values mentioned above we obtain a wall width  $w = 109L_x$ . In figure 4 we show the magnetostatic field normalized to its strength for a VW located at  $z_w = 750L_x$ , whereas figure 5 shows the same plot for the VW confined at the middle of the tube ( $z_w = 500L_x$ ).

Both figures illustrate three regions where there is magnetic charge; upper and lower tube ends, and the region of the DW around the wall position  $z_w$ , which has been highlighted. There are negative surface charges at the tube ends, because  $\sigma_M(0) = -M_z(0) = -M_s < 0$  and  $\sigma_M(L) = M_z(L) = -M_s < 0$ . Also, there is a positive volume charge localized in the domain wall region. A volume magnetic charge [28] is given by  $\rho_M = -\nabla \cdot M$ , and thus in our case  $\rho_M = -\partial M_z / \partial z$ . Besides,  $M_z = M_s \cos \Theta(z)$ , and therefore,  $\rho_M = M_s(\pi/w) \sin \Theta > 0$ , just in the DW region. Therefore, the DW acts as a source of magnetic charge. Note that we are

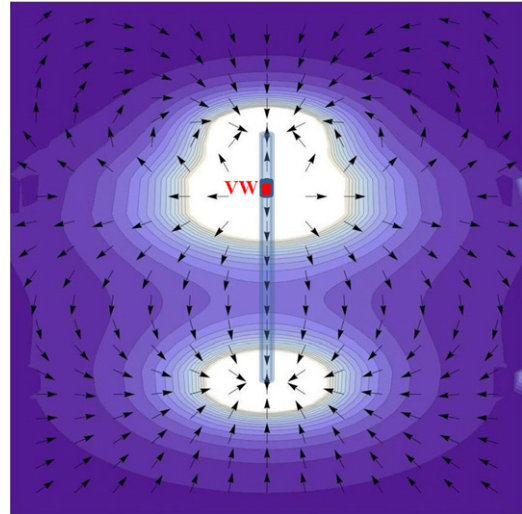


**Figure 4.** Vector plot of the magnetostatic field for a ferromagnetic nanotube with a vortex domain wall located at  $z_w = 750L_x$ . White regions indicate where the magnetostatic field is stronger, as occurs around the DW and at the tube ends. Parameters are presented in the main text. (Colour online.)

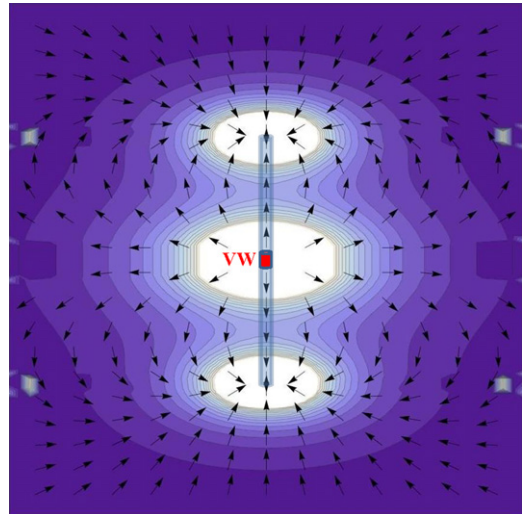


**Figure 5.** Vector plot of the magnetostatic field for a ferromagnetic nanotube with a vortex domain wall located at  $z_w = 500L_x$ . White regions indicate a stronger magnetostatic field. Parameters are presented in the text. (Colour online.)

considering here head-to-head DWs, and in order to analyze the case of tail-to-tail walls, we should replace  $M_z$  by  $-M_z$  and the corresponding magnetic charges must have the opposite sign as discussed here for head-to-head walls.

Finally, in figure 6 we illustrate the strength of the dipolar field as a function of the distance to the  $z$ -axis, and for different  $z$  values. We have considered the same parameters as in figure 5, which means that we have magnetic matter just for  $\rho/L_x = 9-10$  and  $z/L_x = 0-1000$ .

### 3.3. Vector plots for a TW

To visualize the magnetostatic field produced by a TW, we have chosen MNs with the same parameters as in the above section, that is  $\beta = 0.9$ ,  $L = 1000L_x$  and  $R = 10L_x$ . Following a

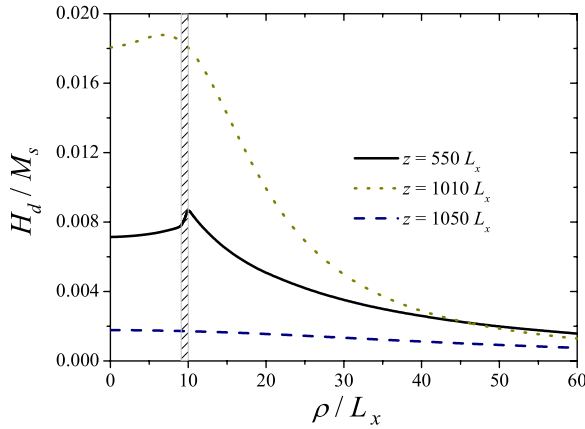


**Figure 6.** Strength of the magnetostatic field for a MN with a vortex domain wall located at  $z_w/L_x = 500$ . Parameters are the same as figure 5 while the dashed region represents the region occupied by the magnetic matter. (Colour online.)

previous work [19] we can calculate the transverse DW width ( $w$ ) by minimizing the total energy, as stated before. Again, it is found that  $w = w(\beta, R)$ , and for the above mentioned values we obtain  $w = 7.67L_x$ , a rather small value as compared with the corresponding DW width for the VW of the above section. The magnetic field for the TW configuration is given by equations (14)–(16). Note that the angular component of the field  $H_\phi$  is not zero (unless  $\sin \phi = 0$ ) and therefore the field does not present azimuthal symmetry as the magnetostatic field for the vortex DW. It can be shown that for the geometry discussed here, the vector field along the plane defined by  $\phi = 0$  lies completely in that plane, where  $H_\phi(\phi = 0) = 0$ . Along this plane it is found that the field is very similar to the field for the VW (see figure 5). This can be understood by noting that, mathematically, the field for the TW is very similar to the case of the VW. The main differences are the wall width and the term dependent on the angle  $\phi$  and the function  $A(\rho, z)$  defined in (17).

In figures 7 and 8 we show the magnetostatic field produced by the magnetization of a transverse DW located at  $z_w = 500L_x$ . Figure 7 depicts the top view of the field along the plane  $z = 600L_x$  and figure 8 shows the plane  $z = 1200L_x$ . Both plots represent the in-plane component of the field ( $H_\rho^{TW} \hat{\rho} + H_\phi^{TW} \hat{\phi}$ ) normalized to their strengths given by the colour code. The central ring illustrates the top view of the nanotube. We have also included information about  $H_z^{TW}$  which is given by the length of the arrows. It can be noted that near the ferromagnetic tube, the  $z$  component of the field is more important, and thus the arrows are smaller.

#### 4. Final remarks

In summary, we have investigated the magnetostatic field produced by equilibrium states and non-equilibrium domain wall states of magnetic nanotubes. Using a continuous model we have obtained simple expressions to evaluate the dipolar fields. On the one hand, we can conclude that the consideration of magnetic states as the non-uniform mixed state instead of the

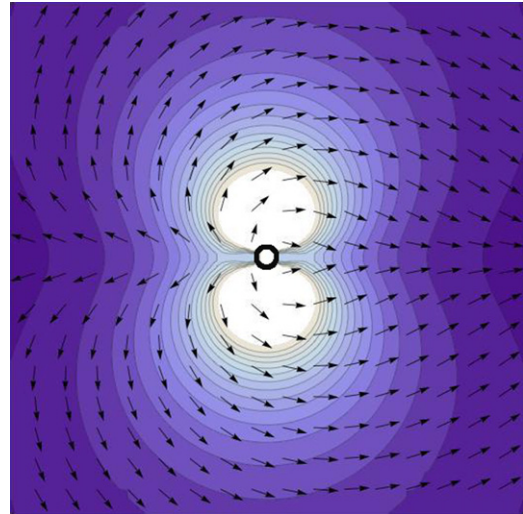


**Figure 7.** Magnetostatic field for a ferromagnetic nanotube with a transverse domain wall located at the middle of the tube ( $z_w = 500L_x$ ). The plot represents the top view of the field, at the plane  $z = 600L_x$ . White regions indicate a stronger magnetostatic field, and along the contours the value of the field is constant. Parameters are presented in the text. (Colour online.)

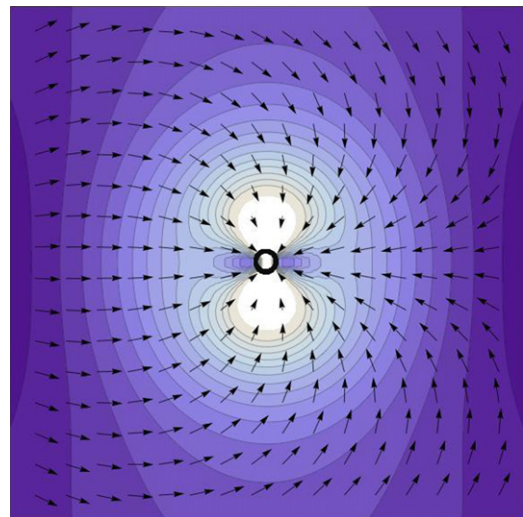


**Figure 8.** Magnetostatic field for a ferromagnetic nanotube with a transverse DW located at the middle of the tube. The plot represents the top view of the field at the plane  $z = 1200L_x$ . White regions indicate a stronger magnetostatic field. Along the contours the value of the field is constant. Parameters are presented in the text. (Colour online.)

idealized uniform state considerably reduces the magnetostatic field. Therefore, it is important for researchers to bear in mind this approach when they compare with experimental results, in order to avoid the overestimation of stray fields. On the other hand, magnetic domain walls, which can be manipulated by external fields or spin-currents, introduce volumetric magnetic charges into the nanostructure. Finally, we have concluded that the magnetostatic field strongly depends on the mechanisms of magnetization reversal. Our results are intended to provide guidelines to use the magnetostatic field generated by tubular nanostructures in prospective applications such as the generation of a magnetic trap.

## Acknowledgments

This work was partially supported by the FONDECYT Grants No 11080246 and 11070010, Financiamiento Basal para Centros Científicos y Tecnológicos de Excelencia, Millennium Science Initiative under Project P06-022-F and the programme 'Bicentenario en Ciencia y Tecnología' PBCT under project PSD-031.

## References

- [1] Wolf S A, Awschalom D D, Buhrman R A, Daughton J M, von Molnar S, Roukes M L, Chtchelkanova A Y and Treger D M 2001 *Science* **294** 1488
- [2] Gerrits Th, van den Berg H A M, Hohlfeld J, Bar L and Rasing Th 2002 *Nature* **418** 509
- [3] Emerich D F and Thanos C G 2003 *Expert Opin. Biol. Ther.* **3** 655
- [4] Lee D, Cohen R E and Rubner M F 2007 *Langmuir* **23** 123
- [5] Eisenstein M 2005 *Nature Methods* **2** 484
- [6] Son S J, Reichel J, He B, Schushman M and Lee S B 2005 *J. Am. Chem. Soc.* **127** 7316
- [7] Nielsch K, Castano F J, Matthias S, Lee W and Ross C A 2005 *Adv. Eng. Mater.* **7** 217
- [8] Wang Z K *et al* 2005 *Phys. Rev. Lett.* **94** 137208
- [9] Tao F, Guan M, Jiang Y, Zhu J, Xu Z and Xue Z 2006 *Adv. Mater. (Weinheim, Germany)* **18** 2161
- [10] Hertel R and Kirschner J 2004 *J. Magn. Mater.* **278** L291
- [11] Daub M, Knez M, Gosele U and Nielsch K 2007 *J. Appl. Phys.* **101** 09J111
- [12] Escrig J, Landeros P, Altbir D, Vogel E E and Vargas P 2007 *J. Magn. Mater.* **308** 233
- [13] Escrig J, Landeros P, Altbir D and Vogel E E 2007 *J. Magn. Mater.* **310** 2448
- [14] Landeros P, Suarez O J, Cuchillo A and Vargas P 2009 *Phys. Rev. B* **79** 024404
- [15] Lee J, Suess D, Schrefl T, Hwan Oh K and Fidler J 2007 *J. Magn. Mater.* **310** 2445
- [16] Chen A P, Usov N A, Blanco J M and Gonzalez J 2007 *J. Magn. Mater.* **316** e317
- [17] Atkinson D, Allwood A, Xiong G, Cooke M D, Faulkner C C and Cowburn R P 2003 *Nature Mater.* **2** 85
- [18] Thomas L, Hayashi M, Jiang X, Moriya R, Retener C and Parkin S S P 2006 *Nature* **443** 197
- [19] Landeros P, Allende S, Escrig J, Salcedo E, Altbir D and Vogel E E 2007 *Appl. Phys. Lett.* **90** 102501
- [20] Escrig J, Bachmann J, Jing J, Daub M, Altbir D and Nielsch K 2008 *Phys. Rev. B* **77** 214421
- [21] Allende S, Escrig J, Altbir D, Salcedo E and Bahiana M 2008 *Eur. Phys. J. B* **66** 37
- [22] Bachmann J, Escrig J, Pitzschel K, Moreno J M M, Jing J, Gorlitz D, Altbir D and Nielsch K 2009 *J. Appl. Phys.* **105** 07B521
- [23] Escrig J, Allende S, Altbir D and Bahiana M 2008 *Appl. Phys. Lett.* **93** 023101
- [24] Pereira A, Denardin J C and Escrig J 2009 *J. Appl. Phys.* **105** 083903
- [25] Escrig J, Allende S, Altbir D, Bahiana M, Torrejon J, Badini G and Vazquez M 2009 *J. Appl. Phys.* **105** 023907
- [26] Klaui M, Vaz C A F, Lopez-Diaz L and Bland J A C 2003 *J. Phys.: Condens. Matter* **15** R985
- [27] Castaño F J, Ross C A, Eilez A, Jung W and Frandsen C 2004 *Phys. Rev. B* **69** 144421
- [28] Aharoni A 1996 *Introduction to the Theory of Ferromagnetism* (Oxford: Clarendon)
- [29] Kravchuk V P, Sheka D D and Gaididei Yu B 2006 *J. Magn. Mater.* **310** 116
- [30] Landeros P, Escrig J and Altbir D 2009 *Electromagnetic, Magnetostatic, and Exchange-interaction Vortices in Confined Magnetic Structures* ed E O Kamenetskii (Kerala: Research Signpost)
- [31] Beleggia M, Lau J W, Schofield M A, Zhu Y, Tandon S and De Graef M 2006 *J. Magn. Mater.* **301** 131